ORIGINAL ARTICLE

Identification of MAGI1 as a tumor-suppressor protein induced by cyclooxygenase-2 inhibitors in colorectal cancer cells

J Zaric[1,2,3], J-M Joseph[4], S Tercier[4], T Sengstag[5,6], L Ponsonnet[1,2], M Delorenzi[3,5] and C Rüegg[1,2,3]

[1]Division of Experimental Oncology, Multidisciplinary Oncology Center (CePO), University Medical Center (CHUV), University of Lausanne (UNIL), Lausanne, Switzerland; [2]Pathology, Department of Medicine, Faculty of Science, University of Fribourg (UNIFR), Fribourg, Switzerland; [3]National Center for Competence in Research (NCCR), Molecular Oncology, Swiss Institute for Experimental Cancer Research (ISREC)-Ecole Polytechnique Fédérale de Lausanne (EPFL), Lausanne, Switzerland; [4]Department of Pediatric Surgery, University Medical Center (CHUV), University of Lausanne (UNIL), Lausanne, Switzerland and [5]Swiss Institute of Bioinformatics (SIB), Lausanne, Switzerland

Cyclooxyganase-2 (COX-2), a rate-limiting enzyme in the prostaglandin synthesis pathway, is overexpressed in many cancers and contributes to cancer progression through tumor cell-autonomous and paracrine effects. Regular use of non-steroidal anti-inflammatory drugs or selective COX-2 inhibitors (COXIBs) reduces the risk of cancer development and progression, in particular of the colon. The COXIB celecoxib is approved for adjunct therapy in patients with Familial adenomatous polyposis at high risk for colorectal cancer (CRC) formation. Long-term use of COXIBs, however, is associated with potentially severe cardiovascular complications, which hampers their broader use as preventive anticancer agents. In an effort to better understand the tumor-suppressive mechanisms of COXIBs, we identified MAGUK with Inverted domain structure-1 (MAGI1), a scaffolding protein implicated in the stabilization of adherens junctions, as a gene upregulated by COXIB in CRC cells and acting as tumor suppressor. Overexpression of MAGI1 in CRC cell lines SW480 and HCT116 induced an epithelial-like morphology; stabilized E-cadherin and β-catenin localization at cell–cell junctions; enhanced actin stress fiber and focal adhesion formation; increased cell adhesion to matrix proteins and suppressed Wnt signaling, anchorage-independent growth, migration and invasion *in vitro*. Conversely, MAGI1 silencing decreased E-cadherin and β-catenin localization at cell–cell junctions; disrupted actin stress fiber and focal adhesion formation; and enhanced Wnt signaling, anchorage-independent growth, migration and invasion *in vitro*. MAGI1 overexpression suppressed SW480 and HCT116 subcutaneous primary tumor growth, attenuated primary tumor growth and spontaneous lung metastasis in an orthotopic model of CRC, and decreased the number and size of metastatic nodules in an experimental model of lung metastasis.

Correspondence: Professor C Rüegg, Pathology, Department of Medicine, Faculty of Science, University of Fribourg (UNIFR), 1, Rue Albert Gockel, Fribourg CH-1700, Switzerland.
E-mail: curzio.ruegg@unifr.ch
[6]Current address: OSC—Omics Science Center, RIKEN Yokohama Institute, 1-7-22 Suehirocho, Tsurumiku, Yokohama 230-0045, Japan

Collectively, these results identify MAG1 as a COXIB-induced inhibitor of the Wnt/β-catenin signaling pathway, with tumor-suppressive and anti-metastatic activity in experimental colon cancer.

Introduction

Colorectal cancer (CRC) development is a multistep process (Ilyas *et al.*, 1999). Activation of the Wnt/β-catenin pathway is considered as a critical initiating event in the majority of human CRCs (Fodde and Brabletz, 2007). The Wnt/β-catenin pathway is negatively regulated by the adenomatous polyposis coli (APC) tumor-suppressor protein, which targets β-catenin to proteosomal degradation, and by the cell–cell adhesion molecule E-cadherin, which sequesters β-catenin to the cell membrane. The Wnt/β-catenin pathway can be activated through inhibition of β-catenin degradation or loss of E-cadherin, thereby causing the accumulation of β-catenin in the cytoplasm and its translocation to the nucleus. In the nucleus, β-catenin forms a complex with the T-cell factor/lymphoid enhancer-binding factor-1 (TCF/LEF1) transcription factor to control gene expression (Clevers, 2006). Familial adenomatous polyposis patients have APC mutations preventing β-catenin degradation, and develop multiple intestinal polyps progressing to CRC at an early age. At least one APC allele is mutated in about 60% of sporadic CRCs and somatic β-catenin mutations are found in 50% of CRCs with wild-type (WT) APC alleles, further emphasizing the importance of the Wnt/β-catenin pathway in CRC development (Fodde and Brabletz, 2007).

A significant increase in cyclooxygenase-2 (COX-2, also known as PTGS2) levels occurs during colorectal carcinogenesis (Gupta, 2001). Epidemiological studies showed that regular intake of non-steroidal anti-

inflammatory drugs (for example, aspirin) or selective COX-2 inhibitors (COXIBs, for example, celecoxib) decreases the risk of developing CRC (Wang and Dubois, 2006). Celecoxib (2×400 mg/day) was shown to significantly reduce the number of colorectal and duodenal polyps in familial adenomatous polyposis patients (Steinbach et al., 2000), and is now approved as adjunctive therapy to decrease the risk of CRC development in familial adenomatous polyposis patients (Bertagnolli et al., 2009). Long-term use of high doses of COXIBs as chemopreventive strategy in sporadic CRC, however, is not recommended because of the elevated risk of potentially severe cardiovascular complications (Cuzick et al., 2009).

The Membrane-Associated Guanylate Kinase (MA-GUK) family member with Inverted domain structure-1 (MAGI1) consists of six PSD95/DiscLarge/ZO-1 (PDZ) domains, a guanylate kinase domain and two WW domains flanked by two PDZ domains (Dobrosotskaya et al., 1997). MAGI1 localizes to cell–cell contacts and acts as a scaffold molecule to stabilize cadherin-mediated adhesions and to recruit molecules at cell–cell contacts in endothelial and epithelial cells (Laura et al., 2002). Through its PDZ domains MAGI1 associates with a variety of PDZ-binding molecules such as N-methyl-D-aspartate receptors (Hirao et al., 1998), δ-catenin (Ide et al., 1999), brain specific angiogenesis inhibitor 1 (BAI-1) (Mino et al., 2000), mNET1 (Dobrosotskaya, 2001), phosphatase and tensin homologue (PTEN) (Kotelevets et al., 2005) and β-catenin (Dobrosotskaya and James, 2000; Kawajiri et al., 2000). In epithelial cells MAGI1 localizes at adherens junctions in complex with β-catenin/E-cadherin (Dobrosotskaya and James, 2000; Kawajiri et al., 2000) as well as at tight junctions (Ide et al., 1999). MAGI1 suppresses the invasiveness of Madin-Darby Canine Kidney (MDCK) cells by recruiting PTEN to cell–cell contacts and decreasing phosphatidylinositol-3-OH kinase signaling (Kotelevets et al., 2005). TRIP6 has been identified as a binding partner of MAGI1b in epithelial cells that promotes MDCK invasiveness through the activation of nuclear factor-κB and Akt (Chastre et al., 2009). Taken together, MAGI1 is an important molecule for the stabilization of cadherin-mediated cell–cell interactions and the suppression of invasiveness in non-transformed epithelial cells.

In an effort to identify COXIBs-regulated genes affecting cancer progression, we have identified MAGI1 as COXIB-induced gene in CRC cells. MAGI1 promotes E-cadherin and β-catenin recruitment to the membrane, and suppresses TCF/LEF1 transcriptional activity. It induces a cohesive epithelial cell phenotype, decreases the migration and invasiveness of CRC cell lines in vitro, and inhibits experimental CRC growth and metastasis in vivo.

Results

COX-2 inhibition increases MAGI1 expression in CRC cells
Using a microarray-based screen in human umbilical vein endothelial cells treated with the COXIB celecoxib,

we have recently identified genes regulated by celecoxib. A total of 105 genes were downregulated with >2-fold difference and 47 genes were upregulated with >2-fold difference (false discovery rate (FDR)<0.05). MAGI1 mRNA was among the induced transcripts (FDR = 0.0047) (J Zaric et al., unpublished data). As COX-2 promotes CRC (CRC) formation and progression (Gupta, 2001), and COXIBs have protective effects, we set up to test whether celecoxib modulated MAGI1 expression in CRC cells. Celecoxib treatment increased MAGI1 mRNA and protein levels in the SW480, HCT116, SW680, T84 and HT29 human CRC-derived
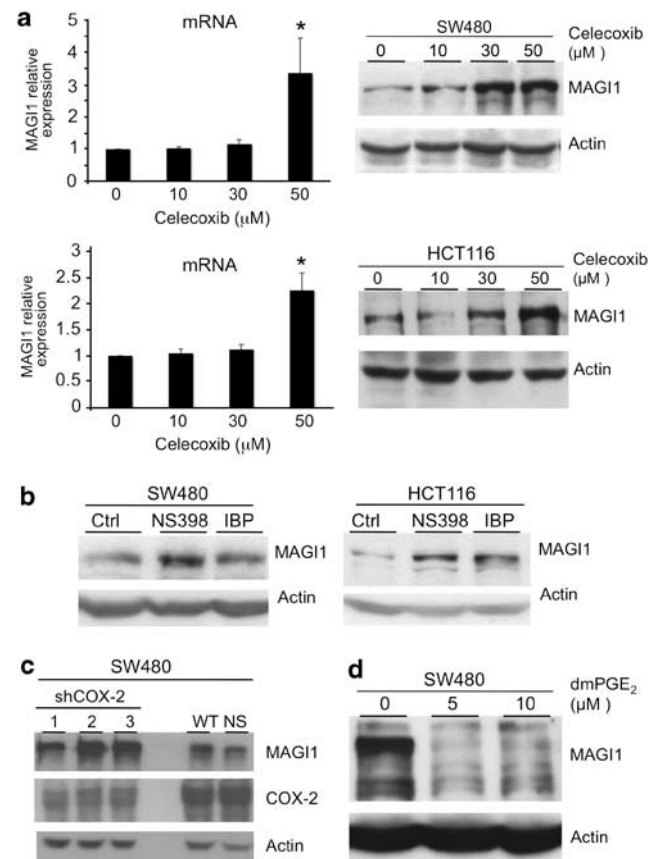

Figure 1 COXIBs induce MAGI1 expression in colorectal carcinoma cells. (a) SW480 and HCT116 cells were cultured for 4 days in the absence or presence of celecoxib at the indicated concentrations. MAGI1 mRNA levels were measured by real-time RT–PCR (left panels) and MAGI1 protein expression was analyzed by western blotting (right panels). Celecoxib treatment induces MAGI1 mRNA and protein expression. *$P<0.001$ compared with the untreated control. (b) SW480 (left panel) and HCT116 (right panel) cells were treated with the COXIB NS398 and the pan-COX-1/2 inhibitor ibuprofen (IBP) for 4 days and subsequently analyzed for MAGI1 protein levels by western blotting. NS398 and IBP treatments induce MAGI1 protein expression. (c) Western blotting showing MAGI1 and COX-2 levels in SW480 cells silenced for COX-2 (sh1-3) as compared with WT and non-silenced (NS) control cells. COX-2 silencing enhances MAGI1 protein expression. (d) Western blotting showing reduced MAGI1 protein in SW480 cells exposed to 16,16 dimethyl PGE2 (dmPGE2) for 24 h. COX-2, cyclooxygenase-2; COXIB, COX-2 inhibitor; MAGI1, MAGUK with Inverted domain structure-1; MAGUK, Membrane-Associated Guanylate Kinase; PGE2, prostaglandin-E2; RT–PCR, reverse transcription–PCR; WT, wild type.

cell lines *in vitro* (Figure 1a and Supplementary Figure S1a). MAGI1 was abundant in the DLD1 cell line (Stolfi *et al.*, 2008) expressing only trace amounts of COX-2 protein and mRNA (Supplementary Figures S1b and S1c), and no increase was observed in response to celecoxib (Supplementary Figure S1a). Treatment of SW480 and HCT116 cells with NS-398, another COX-2-specific inhibitor, and ibuprofen, a pan-COX-1/2 inhibitor, also increased the MAGI1 protein level (Figure 1b). Silencing of COX-2 expression in SW480 cells using three different COX-2 short-hairpin RNAs (shRNAs) resulted in increased MAGI1 expression (Figure 1c). SW480 and HCT116 cells express mostly the prostaglandin-E2 (PGE$_2$) receptor EP$_4$ (Supplementary Figure S1d), and treatment of SW480 cells with the stabilized PGE$_2$ analog, 16,16 dimethyl PGE$_2$, resulted in a decrease of MAGI1 protein and mRNA levels (Figure 1d and Supplementary Figure S1e). SW480 and HCT116 cells were used for subsequent experiments.

To obtain evidence that COX-2 also regulates MAGI1 expression *in vivo*, we injected SW480 cells subcutaneously into Swiss nu/nu mice and when tumors were palpable we fed the mice either with a celecoxib-supplemented diet or a conventional diet. Celecoxib treatment significantly reduced tumor growth (Supplementary Figure S2a), consistent with findings in other tumor models (Gupta *et al.*, 2007), and increased MAGI1 levels (Supplementary Figure S2b).

From these results, we conclude that the MAGI1 mRNA and protein are induced by celecoxib in CRC cell lines *in vitro* and in derived tumors *in vivo*, and that PGE$_2$ suppresses MAGI1 expression.

MAGI1 promotes an epithelial morphology and inhibits the migration, invasion and adhesion-independent growth of CRC cells

In order to investigate the effects of MAGI1 in CRC cells, we generated SW480 and HCT116 cells over-expressing MAGI1 or with silenced MAGI1 (Supplementary Figure S3). Parental SW480 cells consist of a mixture of adherent and loosely attached, rounded cells, often overgrowing as cell aggregates (Figure 2a, top row). MAGI1-overexpressing SW480 cells acquired a flattened, epithelial-like morphology, whereas MAGI1-silenced cells acquired a round shape and grew in clusters. Staining for F-actin and paxillin showed cortical actin, stress fibers and paxillin-positive focal adhesions in SW480 WT cells. MAGI1-overexpressing cells have mostly stress fibers and well-formed focal adhesions, whereas MAGI1-silenced cells had no stress fibers, some cortical actin and no paxillin-positive focal adhesions (Figure 2a, middle and lower rows). In MAGI1-overexpressing SW480 cells, E-cadherin localized predominantly at cell–cell junctions, whereas in MAGI1-silenced cells E-cadherin localization at cell–cell contacts was largely lost (Figure 2b). MAGI1 over-expression reduced SW480 cell migration and suppressed Matrigel invasion, whereas MAGI1 silencing facilitated migration and invasion (Figure 2c). Identical results were obtained using HCT116 cells (Supplementary Figure S4a). MAGI1 silencing promoted and

MAGI1 overexpression reduced SW480 anchorage-independent colony formation in an agarose assay (Figure 2d). MAGI1 overexpression or silencing had minor but significant effects on cell growth in two-dimensional conditions (Supplementary Figure S4b).

These results show that MAGI1 reverses the *in vitro* cell-autonomous traits of malignancy in CRC cells, including morphology, motility, invasion and anchorage-dependent growth.

MAGI1 promotes integrin-mediated cell adhesion and signaling

To address whether MAGI1 might modify cell adhesion to extracellular matrix proteins, we performed short-term *in vitro* adhesions assays. MAGI1 overexpression enhanced and MAGI1 silencing decreased SW480 adhesion to collagen-I, fibronectin and laminin (Figure 3a). Enhanced adhesion was not associated with increased cell-surface integrin expression and could be prevented by using anti-integrin function-blocking anti-bodies (Supplementary Figures S5a and S5b). MAGI1 overexpression in SW480 cells enhanced the phosphorylation of focal adhesion kinase (FAK), extracellular signal-regulated kinase-1/2 (ERK1/2) and Akt (Figures 3b and c), three kinases activated by out-side-in integrin signaling (Cabodi *et al.*, 2010). Increased FAK, ERK1/2 and Akt phosphorylation was transient and no longer detectable 60 min after adhesion.

These results show that MAGI1 enhances integrin-mediated cell adhesion and out-side-in signaling.

MAGI1 inhibits Wnt/β-catenin signaling in CRC cells

Activation of the Wnt/β-catenin pathway is considered as an initiating event in human colorectal cancerogenesis (Clevers, 2006). As β-catenin was shown to bind to MAGI1 in adherens junctions in epithelial cells (Dobrosotskaya and James, 2000), we speculated that MAGI1 expression levels might modulate the Wnt/β-catenin pathway. To address this issue, we first analyzed the effect of MAGI1 on the activity of the β-catenin-regulated TCF/LEF1 transcriptional complex using the TCF/LEF1 luciferase reporter system TOPFlash/FOP-Flash. MAGI1 overexpression in SW480 decreased TCF/LEF1 transcriptional activity, whereas MAGI1 silencing increased the same (Figure 4a). Consistent with these results, MAGI1 overexpression reduced axin-2 and c-Myc levels, two β-catenin/TCF/LEF1 target genes, whereas MAGI1 silencing increased their expression (Figures 4b and c and Supplementary Figure S6). In MAGI1-overexpressing SW480 cells β-catenin was predominantly located at the cell membrane, whereas in MAGI1-silenced cells it was diffuse in the cytoplasm (Figure 4d), consistent with the modulation of the Wnt/β-catenin pathway by MAGI1.

Taken together, these results show that MAGI1 inhibits Wnt/β-catenin signaling in CRC cells.

MAGI1 overexpression suppresses tumor cell growth and spontaneous lung metastasis

Next, we tested whether changes in MAGI1 levels might modulate SW480 and HCT116 tumor growth and
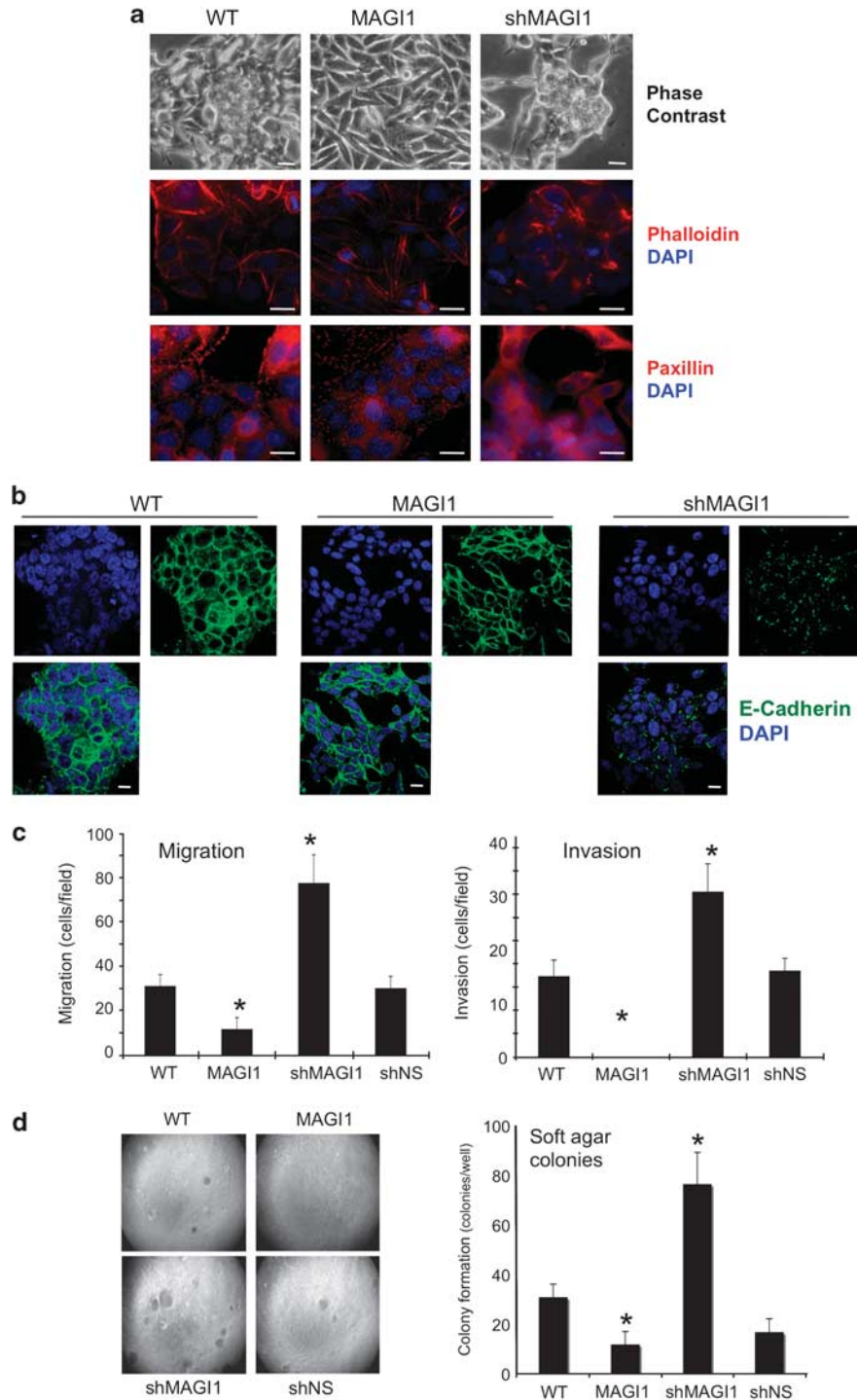
Figure 2 MAGI1 modulates morphology, migration, invasion and anchorage-independent growth. (**a**) Phase-contrast microscopic images (upper row), and immunostaining of F-actin (phalloidin, middle row) and paxillin (paxillin) of WT, MAGI1-overexpressing and MAGI1-silenced SW480 cells. Nuclei were counterstained with 4,6-diamidino-2-phenylindole. MAGI1 overexpression induced a flattened epithelial morphology, actin stress fiber and paxillin-positive focal adhesion formation, whereas MAGI1 silencing caused cell rounding and aggregation, and loss of actin stress fibers and focal adhesions. (**b**) Confocal immunofluorescence imaging showing that in SW480 cells E-cadherin localized both at cell junctions and the cytoplasm. MAGI1 overexpression promoted localization at cell–cell junctions, whereas MAGI1 silencing disrupted E-cadherin localization at cell–cell contacts. (**c**) Effect of MAGI1 overexpression silencing on the cell migration (left panel) and invasion (right panel) of serum-starved SW480 cells. The results represent the average number of cells per field ± s.d. counted on the lower side of the insert membrane. *$P<0.001$ compared with the WT ($n=3$). (**d**) SW480 WT, SW480-overexpressing and SW480-silenced cells grown in soft agar. MAGI1 silencing favors anchorage-independent growth of SW480 cells, whereas MAGI1 overexpression inhibits the same. The quantitative results are expressed on the right as mean value of triplicate determinations ± s.d. *$P<0.05$ compared with the WT ($n=3$). MAGI1, MAGI1-overexpressing; MAGI1, MAGUK with Inverted domain structure-1; MAGUK, Membrane-Associated Guanylate Kinase; shMAGI1, MAGI1-silenced; shNS, non-silenced control; WT, wild type.
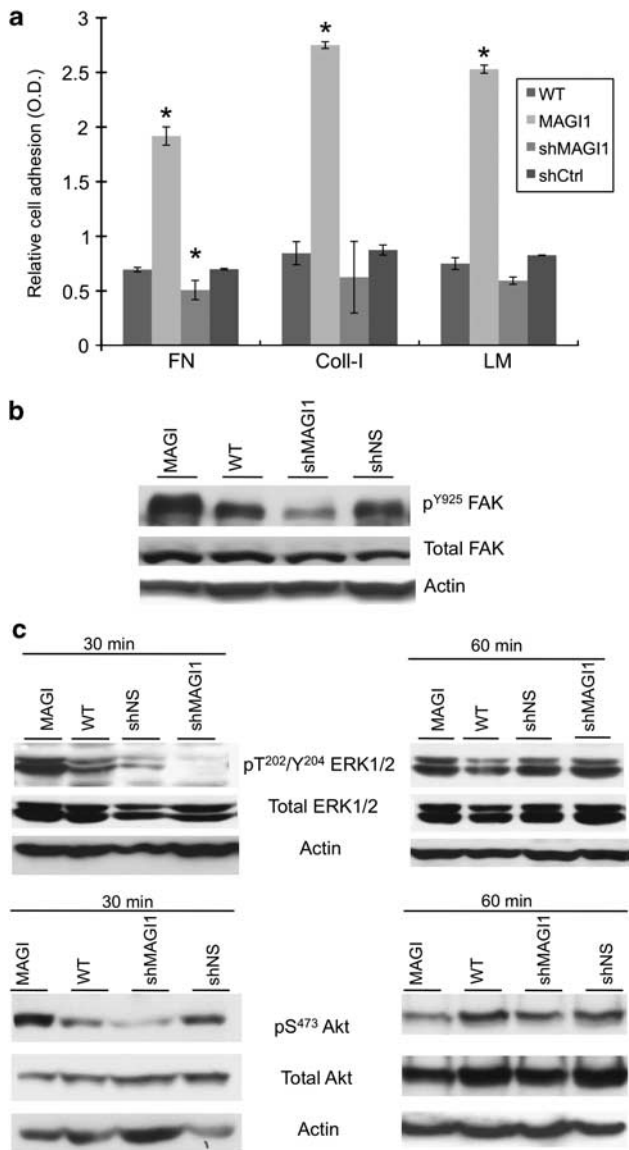
Figure 3 MAGI1 promotes integrin-mediated cell adhesion and signaling. (a) Short-term adhesion assay of WT, MAGI1-over-expressing and MAGI1-silenced SW480 cells on fibronectin, collagen-I and laminin. MAGI1 overexpression strongly enhanced adhesion. The results represent the mean ± s.d. of four replicate experiments. *$P < 0.001$ compared with the WT ($n = 3$). (b) Western blot analysis of Y^{925}-FAK phosphorylation and total FAK of SW480 serum starved for 12 h and left to adhere to collagen-I for 30 min. (c) Western blot analysis of phospho-T^{202}/Y^{204}-ERK1/2 and total ERK1/2, and phospho-S^{473}-Akt and total Akt, of SW480 cells serum starved for 12 h and left to adhere to collagen-I for 30 or 60 min. Actin immunoblotting shows equivalent protein loading across different lanes. WT, wild type; MAGI1, MAGI1-over-expressing; shMAGI1, MAGI1-silenced; shNS, non-silenced control. ERK, extracellular signal-regulated kinase; FAK, focal adhesion kinase; MAGI1, MAGUK with Inverted domain structure-1; MAGUK, Membrane-Associated Guanylate Kinase.

progression by injecting WT, MAGI1-silenced or MAGI1-overexpressing SW480 and HCT116 tumor cells subcutaneously into immunodeficient mice. MAGI1 overexpression strongly suppressed tumor growth, whereas silencing of MAGI1 resulted in a modest increase in tumor size as compared with that of control tumors (Figures 5a and b). Histological analyses of the primary tumors, lungs and livers showed no evidence of local invasion or metastasis (data not shown). To test whether MAGI1 overexpression was essential for the tumor-suppressive effects of celecoxib, we injected mice with SW480 cells non-silenced or silenced for MAGI1 expression and treated one cohort of mice with celecoxib. MAGI1-silenced cells were slightly but significantly ($P < 0.04$) less sensitive to the effect of celecoxib (Figure 5c). This suggests that celecoxib acts through MAGI1-dependent and MAGI1-independent mechanisms. One possible MAGI1-independent mechanism is inhibition of angiogenesis (Gupta and Dubois, 2001). Indeed, microvascular density was decreased in celecoxib-treated tumors, regardless of the MAGI1 status (Supplementary Figure S7a).

As subcutaneous transplantation models are not well suited for studying metastasis, we interrogated the role of MAGI1 on metastasis formation using an orthotopic implantation model (Cespedes et al., 2007). This model produces metastases in almost all clinically relevant sites occurring in human patients: regional and occasionally distal lymph nodes, liver, lungs and peritoneum. Luciferase-expressing WT, MAGI1-overexpressing and MAGI1-silenced SW480 cells were implanted orthotopically in the cecum of NOD/SCIDcγ-null mice (NSG) mice. Luminescence detection showed a 1-log increase in the signal from in MAGI1-silenced SW480 tumors as compared with that from SW480 WT tumors, and a 3-log decrease in the signal from MAGI1-overexpressing SW480 tumors as compared with that from WT tumors (Figure 5d and Supplementary Figure S7b). SW480 tumors metastasized to the lung as detected by the luminescence signal in the thorax region starting week 4 (Figure 6a). MAGI1 overexpression consistently suppressed the luciferase signal fully in the lungs, whereas MAGI1 silencing enhanced the same, however, with great variability (Figure 6a). Histological analysis of lungs, liver and mesenteric tissue confirmed the presence of metastases in the lungs and mesenterium of mice bearing WT and MAGI1-silenced tumors, whereas liver was metastasis-free (Figure 6b and data not shown).

MAGI1 overexpression suppresses experimental SW480 metastasis to the lung
As MAGI1-overexpressing SW480 tumors suppress primary tumor growth, it is possible that the observed reduced formation of spontaneous lung metastases is because of the fact that primary tumors are small. To address this possibility, we injected WT and MAGI1-overexpressing SW480 into the tail vein of mice, and 4 weeks later we analyzed the lungs for the presence of metastases. MAGI1 overexpression significantly decreased both the number of nodules and their size, thereby showing an affect of MAGI1 in metastasis seeding and outgrowth (Figures 6c and d).

In conclusion, SW480 tumor transplantation experiments showed that MAGI1 overexpression suppresses primary tumor growth, metastasis seeding and metastasis growth.
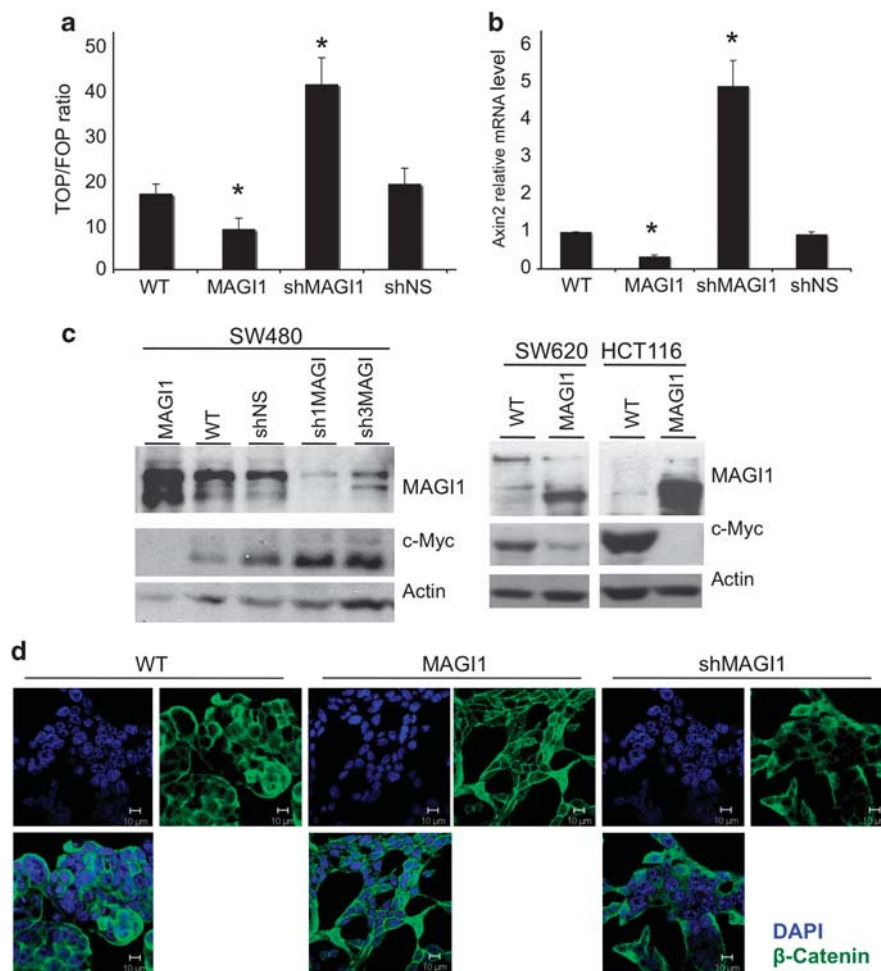
Figure 4 MAGI1 overexpression inhibits Wnt signaling. (**a**) Measurement of TCF/LEF1 transcriptional activity using the TOPFlash/FOPFlash assay in SW80 cells. MAGI1 silencing enhanced TOPFlash activity, whereas MAGI1 overexpression decreased the same. *$P<0.001$ compared with WT ($n=3$). (**b**) Real-time RT–PCR analysis showing that MAGI1 silencing enhances axin-2 mRNA level whereas MAGI1 overexpression decreases the same. The results represent the mean values ± s.d. of fold difference relative to the axin-2 level in WT cells normalized to GAPDH levels. *$P<0.001$ compared with the WT. (**c**) Left panel: Western blot analysis showing that MAGI1 overexpression represses c-Myc expression in SW480 cells, whereas MAGI1 silencing induces the same. Right panel: Western blot analysis of SW680 and HCT116 cells showing that MAGI1 reduces c-Myc expression. Actin immunoblotting shows equivalent protein loading. (**d**) Confocal immunofluorescence images of SW480 cells showing that MAGI1 overexpression promotes β-catenin localization at cell–cell junctions, whereas MAGI1 silencing disrupts the same. WT, wild type; MAGI1, MAGI1-overexpressing; shMAGI1, MAGI1-silenced; shNS, non-silenced control. GAPDH, glyceraldehyde-3-phosphate dehydrogenase; MAGI1, MAGUK with Inverted domain structure-1; MAGUK, Membrane-Associated Guanylate Kinase; RT–PCR, reverse transcription–PCR; TCF/LEF1, T-cell factor/lymphoid enhancer-binding factor-1.

Discussion

Increased colorectal mucosal levels of COX-2 and PGE₂ are observed in colon adenoma and CRC, and are implicated in colorectal carcinogenesis (Gupta, 2001). Two distinct, complementary tumor-promoting effects of COX-2 have been reported. First, COX-2 induces modifications of the tumor stroma, promoting tumor progression (Gupta and Dubois, 2001). For example, COX-2 promotes tumor angiogenesis by stimulating the expression of vascular endothelial growth factor in tumor and stromal cells (Tsujii et al., 1998), enhancing vascular endothelial growth factor mitogenic activity in endothelial cells (Jones et al., 1999) and $\alpha_V\beta_3$-dependent activation of Rac-1 and Cdc42 (Dormond et al., 2001). Second, COX-2 directly stimulates tumor cell survival, proliferation,

migration and invasion in conjunction with oncogenic pathways. For example, activation of HER2/HER3 heterodimers in CRC cells induces COX-2 expression and PGE₂ production (Vadlamudi et al., 1999), which transactivates the epidermal growth factor receptor and activates ERK, resulting in increased cell migration and proliferation (Pai et al., 2002; Shao et al., 2003). COX-2 also cross-talks with the Wnt pathway (Wang et al., 2004). PGE₂ treatment of mice harboring a heterozygous APC mutation (APC min), a murine model of familial adenomatous polyposis, accelerates polyp formation (Sonoshita et al., 2001). PGE₂ was subsequently found to induce the dephosphorylation of β-catenin resulting in increased nuclear translocation and TCF/LEF1 activation through activation of the phosphatidylinositol-3-OH kinase/Akt pathway and inhibition of glycogen synthase
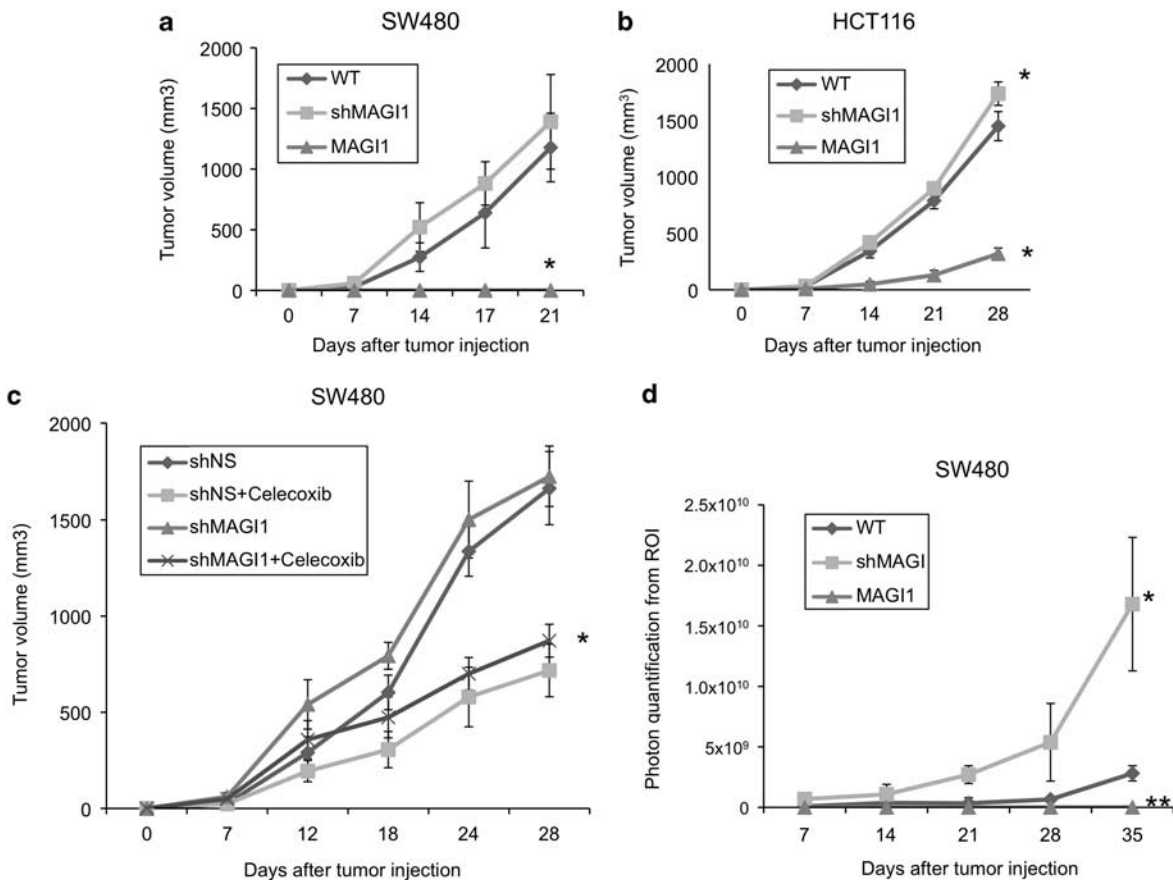
Figure 5 MAGI1 overexpression suppresses subcutaneous and orthotopic SW480 tumor growth. (**a**, **b**) WT, MAGI1-overexpressing and MAGI1-silenced SW480 (**a**) and HCT116 cells (**b**) (1×10^6) were injected subcutaneously into immunocompromised mice. MAGI1 overexpression suppressed tumor growth whereas MAGI1 silencing tended to increase the same. The results represent mean tumor volume ± s.d. (seven mice per group). *$P < 0.05$ compared with the WT. (**c**) MAGI1-silenced SW480 and non-silenced SW480 cells were injected into NSG mice and the mice were maintained on normal diet or a celecoxib-supplemented diet. Celecoxib inhibited both MAGI1-silenced and non-silenced tumors, but MAGI1-silenced tumors were less sensitive. *$P < 0.04$ compared with shNS + celecoxib. (**d**) Luciferase-expressing SW480 cells were injected orthotopically (1×10^6) into the cecum of NSG mice and tumor growth was monitored by detecting *in vivo* luciferase activity. The results represent mean photon values within the tumor region of interest. *$P < 0.05$, **$P < 0.001$ compared with the WT ($n = 2$, 4 mice per group). MAGI1, MAGI1-overexpressing, MAGI1; MAGUK with Inverted domain structure-1; MAGUK, Membrane-Associated Guanylate Kinase; NSG, NOD/SCIDcγ-null mice; shMAGI1, MAGI1-silenced; WT, wild type.

kinase-3β (Castellone *et al.*, 2005; Buchanan and DuBois, 2006). Consistent with such a mechanisms, COX-2 inhibition by celecoxib reduced polyp formation (Swamy *et al.*, 2006). Furthermore, COX-2 itself is a Wnt target (Howe *et al.*, 1999). Expression of Wnt-activating, mutant β-catenin induces COX-2 expression, whereas inhibition of the Wnt pathway by the APC protein suppresses COX-2 expression in CRC cell lines (Araki *et al.*, 2003; Tuynman *et al.*, 2008).

Here we report a previously unrecognized mechanism by which COX-2 inhibition impinges on the Wnt/β-catenin signaling pathway, namely through upregulation of MAGI1, a multi-domain scaffolding molecule present at adherens junctions in complex with E-cadherin/β-catenin. CRC cells treated *in vitro* with the COXIBs celecoxib and NS398, or the pan-COX-1/2 inhibitor ibuprofen, expressed more of the MAGI1 mRNA and protein. The induction of MAGI1 upon COX-2 silencing shows that this activity was not because of the

off-target effects of COXIBs (Abassi *et al.*, 2009). MAGI1 overexpression induced an epithelial-like morphology; stabilized E-cadherin and β-catenin localization at cell–cell junctions; increased paxillin-positive focal adhesions, actin stress fibers and cell adhesion to matrix proteins; and suppressed TCF/LEF1 transcriptional activity, anchorage-independent growth, migration and invasion *in vitro*. MAGI1 silencing decreased E-cadherin localization at cell–cell junctions, disrupted stress fibers and focal adhesions, and enhanced anchorage-independent growth, migration, invasion and TCF/LEF activity *in vitro*. MAGI1 overexpression in tumor cells *in vivo* suppressed primary colorectal tumor growth and lung metastasis formation in an intestinal orthotopic transplantation CRC model and an experimental metastasis model. These observations extend the published data on the activities of MAGI1 in non-transformed cells and uncover a previously unrecognized tumor-suppressive role of MAGI1 in CRC. MAGI1, however, is not the
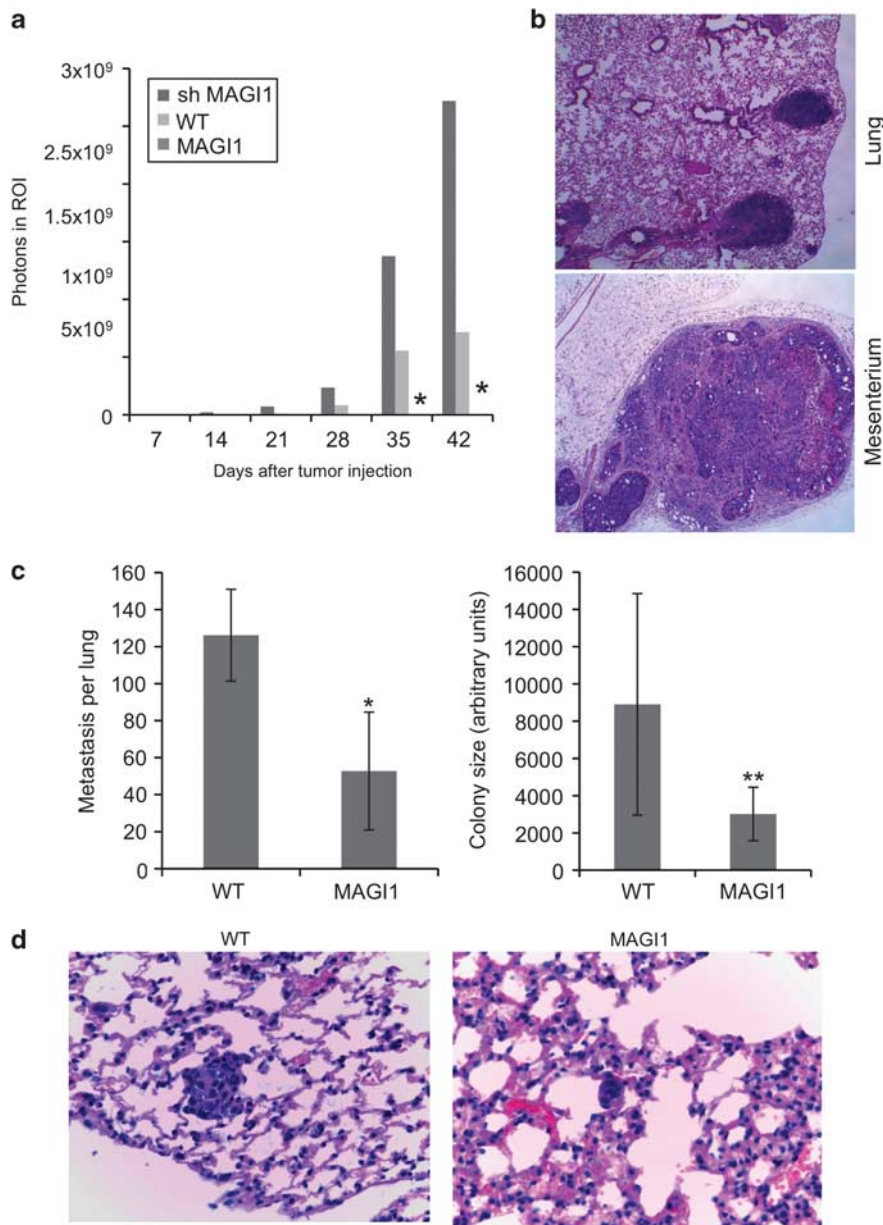
Figure 6 MAGI1 overexpression suppresses metastases formation. (**a**) Spontaneous lung metastasis formation was monitored *in vivo* by luciferase activity over the thorax region in mice bearing orthotopic SW480 tumors. The results represent the mean photon values within the tumor region of interest. MAGI1 overexpression suppresses metastases formation. *$P < 0.05$ compared with the WT ($n = 3$–4). (**b**) Representative histological images (hematoxylin–eosin staining) confirming the presence of metastases in lung and mesenteric tissue. (**c**) Experimental lung metastasis assay. WT and MAGI1-overexpressing cells were injected into the tail vein and mice were killed 4 weeks later. Lung metastases were quantified by counting the number of nodules per lung, and measuring the surface (as surrogate of size) or individual nodules. MAGI1 overexpression suppresses both the number and the size of the metastatic nodules. *$P < 0.01$, **$P < 0.001$ compared with the WT ($n = 7$). (**d**) Representative examples of lung metastases of WT (left) and MAGI1-overexpressing (right) SW480 cells. MAGI1, MAGI1-overexpressing; MAGI1, MAGUK with Inverted domain structure-1; MAGUK, Membrane-Associated Guanylate Kinase; shMAGI1, MAGI1-silenced; WT, wild type.

only mediator of the antitumor activity of celecoxib. Additional mechanisms are involved, as MAGI1 silencing only partially blocked celecoxib from inhibiting tumor growth. Inhibition of tumor-associated angiogenesis is likely to contribute to this effect. In view of the observed phenotypic and functional changes, we considered the possibility that MAGI1 might modulate epithelial-to-mesenchymal transition. We monitored the expression levels of E-cadherin, N-cadherin, vimentin,

Zeb1 and high mobility group AT-hook2 (HMGA2) by immunostaining and reverse transcription (RT)–PCR in MAGI-overexpressing and -silenced SW480 cells but did not observe any differences (data not shown). These results suggest that MAGI1 modulates morphological and functional (that is, invasion and migration) features independently of epithelial-to-mesenchymal transition.

E-cadherin/β-catenin complexes are forming a signalosome that recruits multiple scaffolding molecules such as

MAGI1, PTEN (Kotelevets et al., 2005), Rap1 (Mino et al., 2000) and TRIP6 (Chastre et al., 2009). The stabilization of E-cadherin/β-catenin at the cell–cell borders by MAGI1 overexpression and its loss from cell–cell borders following MAGI1 silencing is consistent with the model that MAGI1 suppresses Wnt/β-catenin signaling by decreasing the pool of free β-catenin. This model is also supported by the published evidence that the COX-2 main product, PGE_2, leads to the inactivation of glycogen synthase kinase-3β, release of β-catenin from the axin/APC complex and its translocation to the nucleus, resulting in the activation of TFC/LEF1-dependent transcription (Castellone et al., 2005; Shao et al., 2005). As tumor cell exposure to PGE_2 results in MAGI1 reduction, it is conceivable that inflammatory and cancer conditions associated PGE_2 production, as it occurs in cancer, may cause a reduction of MAGI1 expression resulting in facilitated Wnt/β-catenin signaling. It will be important to unravel the signaling pathways linking PGE_2/E-prostane receptors to suppressed MAGI1 expression, and identify molecules representing potential therapeutic targets, to maintain high MAGI1 levels under conditions of elevated PGE_2 production as an alternative to COXIBs-based treatments. This could create new opportunities to replace COXIB in pharmacological approaches to prevent CRC in high-risk patients or to treat manifest CRC, thereby potentially avoiding COXIB cardiovascular side effects (Cha and DuBois, 2007). As COX-2 activity suppresses E-cadherin expression in intestinal epithelial cells (Tsujii and DuBois, 1995) and COX-2 inhibition upregulates the same (Noda et al., 2002), it will be important to assess whether there may be a common circuitry that coordinates the disassembling E-cadherin junctional complexes and the promotion of β-catenin/TCF/LEF1 transcriptional activity in response to COX-2 activation. A further question to address is, whether MAGI1 could itself be downregulated by Wnt signaling in CRC cells, thereby creating a self-sustaining loop much alike COX-2, which is both a Wnt-activating protein and a Wnt target gene (Araki et al., 2003; Buchanan and DuBois, 2006). Interestingly, MAGI3 was shown to bind to the Wnt receptors Frizzled-4 and Frizzled-7 (Yao et al., 2004), and to Ltap, a protein homologous to Stbm, which genetically interacts with frizzled to regulate Wnt signaling in Drosophila (Taylor et al., 1998; Wolff and Rubin, 1998). In epithelial cells, MAGI3 and Frizzled-4 form a complex that localizes at cell contact sites (Yao et al., 2004). Taken together, these observations suggest that MAGI1 may be a physiological regulator of Wnt signaling.

In conclusion, we have identified MAGI1 as a COXIB-induced inhibitor of Wnt/β-catenin signaling with tumor- and metastasis-suppressive activity in colon cancer cells.

Materials and methods

Antibodies and chemicals
Bovine serum albumin, paraformaldehyde, poly L-lysine (PLL), fibronectin, laminin, gelatin and collagen-I were purchased from Sigma Chemie (Buchs, Switzerland). The antibodies used are as follows: anti-MAGI1 polyclonal antibody (M5691) and anti-actin monoclonal antibody (mAb), phalloidin–fluorescein isothiocyanate (from Sigma Chemie); anti-paxillin (clone 349) (from Transduction Laboratories, Lexington, KY, USA); anti-c-Myc mAb (sc-40) (from Santa Cruz Biotechnology Inc., Santa Cruz, CA, USA); anti-COX-2 mAb (from Cayman Chemical; Chemie Brunschwig, Basel, Switzerland); anti-β-catenin mAb (from Transduction Laboratories; BD Biosciences, Basel, Switzerland); anti-phospho-Y^{407}-FAK antibody (from Invitrogen, Basel, Switzerland); anti-pY^{925}-FAK, anti-human FAK antibody, anti-phospho-S^{473}-Akt, anti-Akt, anti-ERK1/2 and anti-phospho-T^{202}/Y^{204}-ERK1/2 (from Cell Signaling Technology, Danvers, MA, USA); anti-integrin function-blocking mAbs—mAbs Lia1/2 (anti-β_1), and mAb GI9 (anti-α_2) and GoH3 (anti-α_6) (from Beckman Coulter, Nyon, Switzerland); Sam-1 (anti-α_5) and LM609 (anti-$\alpha_V\beta_3$) (from Millipore, Zug, Switzerland). The biotinylated rat anti-CD31 mAb was from Pharmingen (San Diego, CA, USA). Matrigel was purchased from BD Biosciences, and NS-398 (Futaki et al., 1997) and ibuprofen (Meade et al., 1993) were from Biomol (Enzo Life Sciences, Lausanne, Switzerland). Celecoxib was provided by Pfizer AG (Dübendorf, Switzerland). 16,16 dimethyl PGE_2 was purchased from Cayman (Ann Arbor, MI, USA). D-luciferin was obtained from Caliper Life Sciences (Oftringen, Switzerland).

Cell lines and cell culture
The human colorectal carcinoma cell lines SW480, SW620, HCT116, DLD1, HT29 and T84 were from American Type Culture Collection (LGC Standards, Molsheim, France). For all experiments, cells were grown in high-glucose Dulbecco's modified Eagle's medium (HCT116, HT29 and T84) or RPMI (SW480, SW620 and DLD1) supplemented with 10% fetal calf serum and 1% penicillin/streptomycin, and maintained in a humidified incubator at 37 °C under 5% CO_2. All cell culture reagents were purchased from Invitrogen. Cells were treated with 50 μM Celebrex, 100 μM NS-398 and 50 μM ibuprofen for 4 days (medium with the appropriate drug was changed daily).

In vitro migration and invasion assay
Assays were performed as described previously by Monnier et al. (2008).

Cell adhesion and proliferation assays
Assays were performed as described previously by Zaric and Ruegg (2005) and Bieler et al. (2007).

Soft agar assay
For soft agar assay, 5×10^3 cells were seeded in triplicate in 1 ml of 0.3% (w/v) agar (Difco; BD Biosciences) in complete Dulbecco's modified Eagle's medium (for HCT116) or RPMI (for SW480) medium in six-well plates on 1 ml of a 0.6% bottom agar layer. The cells were fed twice a week and the number of colonies per well was scored 4 weeks later: colonies were counted in four random fields per well under a microscope ($n = 3$). The results are presented as colonies per field and represent the mean values ± s.d.

Luciferase assay
For dual luciferase reporter assays, SW480 and HCT116 cells were transfected with the firefly luciferase reporter constructs (TOPFlash or FOPFlash; Millipore-Upstate, Upstate, MA, USA) and the control Renilla luciferase reporter pRL-TK

(Promega, Dübendorf, Switzerland) using Lipofectamine (Invitrogen). Cells were lysed 48 h after transfection using the cell lysis buffer available in the dual-luciferase reporter assay kit (Promega). Luciferase activity was then measured according to the manufacturer's instructions.

Immunofluorescence microscopy
SW480 cells were cultured when they reached sub-confluence or at confluence on glass coverslips pre-coated with collagen-I (10 μg/ml) placed in 12-well plates in complete RPMI medium for 24–48 h. The cells were then fixed in 4% paraformaldehyde for 10 min at room temperature, permeabilized with 0.1% Triton X-100, blocked with 1% bovine serum albumin and incubated for 1 h with the relevant primary antibodies (5 μg/ml). After washing, the cells were incubated with a Cy5 or fluorescein isothiocyanate-conjugated secondary antibody. 4,6-Diamidino-2-phenylindole was used to counterstain nuclei. The stained cells were mounted in Prolong Antifade medium (Molecular Probes (Basel, Switzerland), Invitrogen) and viewed using a Zeiss LSM 510 Meta confocal microscope (Carl Zeiss AG, Zürich, Switzerland) and DeltaVision Elite (Applied Precision, Issaquah, WA, USA).

Flow cytometric analysis
Stainings, data acquisition and analysis were performed as described previously by Zaric and Ruegg (2005).

Western blot analysis
Cell lysis, sodium dodecyl sulfate–PAGE and blotting were performed as described previously by (Monnier et al. (2008).

RT–PCR and real-time RT–PCR
Total RNA was prepared from cells using RNAsol B (Tel-Test, Inc, Friendswood, TX, USA) and following the manufacturer's instructions. A 5-μg weight of total RNA was reverse-transcribed using random primers (Superscript II; Invitrogen). RT–PCR was performed by cDNA, which was subjected to PCR amplifications using primer pairs specific for EP_1, EP_2, EP_3 and EP_4: EP_1 (NM_000955.2): fw 5′-ACCGACCTGG CGGGCCACCTGA-3′, rev 5′-CGCTGAGCGTGTTGCAC ACCAG-3′; EP_2 (NM_000956.3) fw 5′-TCCAATGACTCC CAGTCTGAGG-3′, rev 5′-TGCATAGATGACAGGCAGC ACG-3′; EP_3 (NM_198717.1) fw 5′-GATCACCATGCTGCT CACTG-3′, rev 5′-AGTTATGCGAAGAGCTAGTCC-3′; EP_4 (NM_000958.2) fw 5′-GGGCTGGCTGTCACCGACC TG-3′, rev 5′-GGTGCGGCGCATGAACTGGCG-3′ (Microsynth, Balgach, Switzerland). The amplification conditions were as follows: 40 cycles of 30 s at 94 °C, 1 min at 62 °C and 1 min at 72 °C.

Real-time PCR was performed using the KAPA SYBR FAST kit (KAPA Biosystems, Boston, MA, USA) and the StepOnePlus machine (Applied Biosystems, Rotkreuz, Switzerland). The primers used were as follows: MAGI1 (NM_001033057) fw 5′-CGTAAAGTGGTTTTTGCGGTGC-3′, rev 5′-TCTCCACGTCGTAGGGCTGC-3′; axin-2 (Koch et al., 2004) fw 5′-GTGCAAACTTTCGCCAACCG-3′, rev 5′-GCTGGTGCAAAGACATAGCC-3′; glyceraldehyde-3-phosphate dehydrogenase (GAPDH) fw 5′-GGACCTGACC TGCCGTCTAG-3′, rev 5′-CCACCACCCTGTTGCTGTAG-3′; COX-2 (PTGS2)(NM_000963.2) fw 5′-GGCGCTCAGC CATACAG-3′, rev 5′-CCGGGTACAATCGCACTTAT-3′, and were purchased from Microsynth. The sample series were run three independent times. The average and standard deviation were calculated for each sample.

Lentiviral constructs
The human MAGI1 cDNA was provided by Dr Y Hata (Department of Medical Biochemistry, Graduate School of Medicine, Tokyo Medical and Dental University, Tokyo, Japan) and sub-cloned into the pRRLSIN.cPPT.PGK/GFP.WPRE lentiviral vector under the control of the phospho glycerate kinase (PGK) promoter (= pSD44 plasmid). For gene silencing experiments, the pCMV-GIN-ZEO lentiviral shRNAmir-expressing system was purchased from Open Biosystems (Huntsville, AL, USA). For the shRNAmir sequences directed against the human MAGI1, three different clones were obtained (clone IDs: V2LHS-36239 (= MAGI1shRNAmir#1)/V2LHS-36236 (= MAGI1shRNAmir#2)/V2LHS-36238 (= MAGI1shRNA mir#3)) that consisted of the shRNAmir sequences cloned into the pSHAG-MAGIC2 (pSM2c) retroviral vector. The three shRNAmir sequences, or a non-silencing control shRNAmir sequence that contains no homology to known mammalian genes, were sub-cloned into the pCMV-GIN-ZEO lentiviral system. For silencing of human COX-2 (PTGS2), three clones were used, with the following clone IDs: V2LHS-6305 (= COX-2shRNAmir#1)/V2LHS-131533 (= COX-2shRNA-mir#2)/V2LHS-131532 (= COX-2shRNAmir#3). The luciferase-expressing lentiviral vector for in vivo cell tracking, pLV-CAG-Luci-IRES-PuroR, was a gift from Dr M Aguet (ISREC-EPFL, Lausanne, Switzerland). Lentiviruses were produced in 293T cells by following the calcium phosphate transfection method by co-transfecting the pCMV-GIN-ZEO constructs or the pSD44-MAGI1 cDNA with the pMD2G plasmid (VSV-G viral envelope construct) and the pMDLgpRRE plasmid. Cell cultures were transduced by overnight incubation at 37 °C in virus-containing media in the presence of 8 μg/ml polybrene. Selection was started on bulk cultures 48 h after transduction using 2 μg/ml puromycin (Sigma Chemie) for the pSD44-MAGI1-cDNA construct or 800 μg/ml G418 (Calbiochem, San Diego, CA, USA) for the pCMV-GIN-ZEO constructs.

In vivo studies
Subcutaneous implantation model. SW480 cells (1×10^6) and derived lines were injected subcutaneously into Swiss nu/nu female mice (6–8 weeks) and HCT116 cells (1×10^6) were injected subcutaneously into NSG mice. Tumor volume was calculated using the following formula: length $\times$ (width)^2 $\times$ 0.52. For celecoxib treatment, mice were randomized at day 7 and assigned to a treated (that is, celecoxib mixed with a powdered rodent chow diet (2018 Global Rodent diet; Harlan Teklad Europe, Lyon, France) at 1000 p.p.m. (= 1g/kg chow) and provided continuously during the course of the experiment) or an untreated group (chow without celecoxib). This protocol allowed attaining celecoxib serum concentrations that are clinically relevant as shown previously by Jacoby et al. (2000) and Gupta et al. (2007).

Orthotopic transplantation model. SW480 cells were tagged with firefly luciferase using lentiviral transduction. The cecum was exteriorized by laparotomy and 1×10^6 cells in 20 μl of Matrigel/RPMI solution were injected into a single spot in the cecal wall using a Hamilton syringe under binocular guidance. The injected cecum was returned to the abdominal cavity and the wound was sutured. The development of primary tumors and metastatic spread was monitored weekly using the IVIS Xenogen Imaging System (Caliper Life Sciences) after intra-peritoneal injection of 150 mg/kg D-luciferin. The results are expressed as photon emission within the 'region of interest'.

Experimental metastasis model. SW480 cells (1×10^6) were injected into the tail vein of 10-week-old NSG females. The

mice were killed 4 weeks later and serial sections of paraffin-embedded lungs were hematoxylin–eosin-stained. The number of metastases was quantified by counting nodules manually and quantifying the surface (using the ImageJ software; NIH) of six sections per lung per animal. The results are presented as the average of the number of metastasis per lung ± s.d. and surface of individual metastasis ± s.d. (in arbitrary values).

Histopathological and immunohistochemical analyses
Standard hematoxylin–eosin staining procedures were performed on paraffin-embedded tissues. For immunohistochemical detection of micro-vessels, tissue was stained with biotinylated rat anti-mouse CD31 as described earlier by Monnier *et al.* (2008).

Statistical analysis
Statistical significance was determined by Student's *t*-test. *P*-value <0.05 was considered significant.

References

Abassi YA, Xi B, Zhang W, Ye P, Kirstein SL, Gaylord MR *et al.* (2009). Kinetic cell-based morphological screening: prediction of mechanism of compound action and off-target effects. *Chem Biol* **16**: 712–723.

Araki Y, Okamura S, Hussain SP, Nagashima M, He P, Shiseki M *et al.* (2003). Regulation of cyclooxygenase-2 expression by the Wnt and ras pathways. *Cancer Res* **63**: 728–734.

Bertagnolli MM, Eagle CJ, Zauber AG, Redston M, Breazna A, Kim K *et al.* (2009). Five-year efficacy and safety analysis of the Adenoma Prevention with Celecoxib Trial. *Cancer Prev Res (Phila, Pa)* **2**: 310–321.

Bieler G, Hasmim M, Monnier Y, Imaizumi N, Ameyar M, Bamat J *et al.* (2007). Distinctive role of integrin-mediated adhesion in TNF-induced PKB/Akt and NF-kappaB activation and endothelial cell survival. *Oncogene* **26**: 5722–5732.

Buchanan FG, DuBois RN. (2006). Connecting COX-2 and Wnt in cancer. *Cancer Cell* **9**: 6–8.

Cabodi S, Di Stefano P, Leal Mdel P, Tinnirello A, Bisaro B, Morello V *et al.* (2010). Integrins and signal transduction. *Adv Exp Med Biol* **674**: 43–54.

Castellone MD, Teramoto H, Williams BO, Druey KM, Gutkind JS. (2005). Prostaglandin E2 promotes colon cancer cell growth through a Gs–axin–beta-catenin signaling axis. *Science* **310**: 1504–1510.

Cespedes MV, Espina C, Garcia-Cabezas MA, Trias M, Boluda A, Gomez del Pulgar MT *et al.* (2007). Orthotopic microinjection of human colon cancer cells in nude mice induces tumor foci in all clinically relevant metastatic sites. *Am J Pathol* **170**: 1077–1085.

Cha YI, DuBois RN. (2007). NSAIDs and cancer prevention: targets downstream of COX-2. *Annu Rev Med* **58**: 239–252.

Chastre E, Abdessamad M, Kruglov A, Bruyneel E, Bracke M, Di Gioia Y *et al.* (2009). TRIP6, a novel molecular partner of the MAGI-1 scaffolding molecule, promotes invasiveness. *FASEB J* **23**: 916–928.

Clevers H. (2006). Wnt/beta-catenin signaling in development and disease. *Cell* **127**: 469–480.

Cuzick JF BJ, Brown PH, Burn J, Greenwald P, Jankowski J, La Vecchia C, Meyskens F, Senn HJ, Thun M. (2009). Aspirin and non-steroidal anti-inflammatory drugs for cancer prevention: an international consensus statement. *Lancet Oncol* **10**: 501–507.

Dobrosotskaya I, Guy RK, James GL. (1997). MAGI-1, a membrane-associated guanylate kinase with a unique arrangement of protein–protein interaction domains. *J Biol Chem* **272**: 31589–31597.

Dobrosotskaya IY. (2001). Identification of mNET1 as a candidate ligand for the first PDZ domain of MAGI-1. *Biochem Biophys Res Commun* **283**: 969–975.

Dobrosotskaya IY, James GL. (2000). MAGI-1 interacts with beta-catenin and is associated with cell–cell adhesion structures. *Biochem Biophys Res Commun* **270**: 903–909.

Dormond O, Foletti A, Paroz C, Ruegg C. (2001). NSAIDs inhibit alpha V beta 3 integrin-mediated and Cdc42/Rac-dependent endothelial-cell spreading, migration and angiogenesis. *Nat Med* **7**: 1041–1047.

Fodde R, Brabletz T. (2007). Wnt/beta-catenin signaling in cancer stemness and malignant behavior. *Curr Opin Cell Biol* **19**: 150–158.

Futaki N, Takahashi S, Kitagawa T, Yamakawa Y, Tanaka M, Higuchi S. (1997). Selective inhibition of cyclooxygenase-2 by NS-398 in endotoxin shock rats *in vivo*. *Inflamm Res* **46**: 496–502.

Gupta GP, Nguyen DX, Chiang AC, Bos PD, Kim JY, Nadal C *et al.* (2007). Mediators of vascular remodelling co-opted for sequential steps in lung metastasis. *Nature* **446**: 765–770.

Gupta RA DR. (2001). Colorectal cancer prevention and treatment by inhibition of cyclooxygenase-2. *Nat Rev Cancer* **1**: 11–21.

Gupta RA, Dubois RN. (2001). Colorectal cancer prevention and treatment by inhibition of cyclooxygenase-2. *Nat Rev Cancer* **1**: 11–21.

Hirao K, Hata Y, Ide N, Takeuchi M, Irie M, Yao I *et al.* (1998). A novel multiple PDZ domain-containing molecule interacting with *N*-methyl-D-aspartate receptors and neuronal cell adhesion proteins. *J Biol Chem* **273**: 21105–21110.

Howe LR, Subbaramaiah K, Chung WJ, Dannenberg AJ, Brown AM. (1999). Transcriptional activation of cyclooxygenase-2 in Wnt-1-transformed mouse mammary epithelial cells. *Cancer Res* **59**: 1572–1577.

Ide N, Hata Y, Nishioka H, Hirao K, Yao I, Deguchi M *et al.* (1999). Localization of membrane-associated guanylate kinase (MAGI)-1/BAI-associated protein (BAP) 1 at tight junctions of epithelial cells. *Oncogene* **18**: 7810–7815.

Ilyas M, Straub J, Tomlinson IP, Bodmer WF. (1999). Genetic pathways in colorectal and other cancers. *Eur J Cancer* **35**: 1986–2002.

Jacoby RF, Seibert K, Cole CE, Kelloff G, Lubet RA. (2000). The cyclooxygenase-2 inhibitor celecoxib is a potent preventive and therapeutic agent in the min mouse model of adenomatous polyposis. *Cancer Res* **60**: 5040–5044.

Jones MK, Wang H, Peskar BM, Levin E, Itani RM, Sarfeh IJ *et al.* (1999). Inhibition of angiogenesis by nonsteroidal anti-inflammatory drugs: insight into mechanisms and implications for cancer growth and ulcer healing. *Nat Med* **5**: 1418–1423.

Kawajiri A, Itoh N, Fukata M, Nakagawa M, Yamaga M, Iwamatsu A et al. (2000). Identification of a novel beta-catenin-interacting protein. *Biochem Biophys Res Commun* **273**: 712–717.

Koch A, Weber N, Waha A, Hartmann W, Denkhaus D, Behrens J et al. (2004). Mutations and elevated transcriptional activity of conductin (AXIN2) in hepatoblastomas. *J Pathol* **204**: 546–554.

Kotelevets L, van Hengel J, Bruyneel E, Mareel M, van Roy F, Chastre E. (2005). Implication of the MAGI-1b/PTEN signalosome in stabilization of adherens junctions and suppression of invasiveness. *FASEB J* **19**: 115–117.

Laura RP, Ross S, Koeppen H, Lasky LA. (2002). MAGI-1: a widely expressed, alternatively spliced tight junction protein. *Exp Cell Res* **275**: 155–170.

Meade EA, Smith WL, DeWitt DL. (1993). Differential inhibition of prostaglandin endoperoxide synthase (cyclooxygenase) isozymes by aspirin and other non-steroidal anti-inflammatory drugs. *J Biol Chem* **268**: 6610–6614.

Mino A, Ohtsuka T, Inoue E, Takai Y. (2000). Membrane-associated guanylate kinase with inverted orientation (MAGI)-1/brain angiogenesis inhibitor 1-associated protein (BAP1) as a scaffolding molecule for Rap small G protein GDP/GTP exchange protein at tight junctions. *Genes Cells* **5**: 1009–1016.

Monnier Y, Farmer P, Bieler G, Imaizumi N, Sengstag T, Alghisi GC et al. (2008). CYR61 and alphaVbeta5 integrin cooperate to promote invasion and metastasis of tumors growing in preirradiated stroma. *Cancer Res* **68**: 7323–7331.

Noda M, Tatsumi Y, Tomizawa M, Takama T, Mitsufuji S, Sugihara H et al. (2002). Effects of etodolac, a selective cyclooxygenase-2 inhibitor, on the expression of E-cadherin–catenin complexes in gastrointestinal cell lines. *J Gastroenterol* **37**: 896–904.

Pai R, Soreghan B, Szabo IL, Pavelka M, Baatar D, Tarnawski AS. (2002). Prostaglandin E2 transactivates EGF receptor: a novel mechanism for promoting colon cancer growth and gastrointestinal hypertrophy. *Nat Med* **8**: 289–293.

Shao J, Jung C, Liu C, Sheng H. (2005). Prostaglandin E2 Stimulates the beta-catenin/T cell factor-dependent transcription in colon cancer. *J Biol Chem* **280**: 26565–26572.

Shao J, Lee SB, Guo H, Evers BM, Sheng H. (2003). Prostaglandin E2 stimulates the growth of colon cancer cells via induction of amphiregulin. *Cancer Res* **63**: 5218–5223.

Sonoshita M, Takaku K, Sasaki N, Sugimoto Y, Ushikubi F, Narumiya S et al. (2001). Acceleration of intestinal polyposis through prostaglandin receptor EP2 in Apc(Delta 716) knockout mice. *Nat Med* **7**: 1048–1051.

Steinbach G, Lynch PM, Phillips RK, Wallace MH, Hawk E, Gordon GB et al. (2000). The effect of celecoxib, a cyclooxygenase-2 inhibitor, in familial adenomatous polyposis. *N Engl J Med* **342**: 1946–1952.

Stolfi C, Fina D, Caruso R, Caprioli F, Sarra M, Fantini MC et al. (2008). Cyclooxygenase-2-dependent and -independent inhibition of proliferation of colon cancer cells by 5-aminosalicylic acid. *Biochem Pharmacol* **75**: 668–676.

Swamy MV, Patlolla JM, Steele VE, Kopelovich L, Reddy BS, Rao CV. (2006). Chemoprevention of familial adenomatous polyposis by low doses of atorvastatin and celecoxib given individually and in combination to APCM in mice. *Cancer Res* **66**: 7370–7377.

Taylor J, Abramova N, Charlton J, Adler PN. (1998). Van Gogh: a new *Drosophila* tissue polarity gene. *Genetics* **150**: 199–210.

Tsujii M, DuBois RN. (1995). Alterations in cellular adhesion and apoptosis in epithelial cells overexpressing prostaglandin endoperoxide synthase 2. *Cell* **83**: 493–501.

Tsujii M, Kawano S, Tsuji S, Sawaoka H, Hori M, DuBois RN. (1998). Cyclooxygenase regulates angiogenesis induced by colon cancer cells. *Cell* **93**: 705–716.

Tuynman JB, Vermeulen L, Boon EM, Kemper K, Zwinderman AH, Peppelenbosch MP et al. (2008). Cyclooxygenase-2 inhibition inhibits c-Met kinase activity and Wnt activity in colon cancer. *Cancer Res* **68**: 1213–1220.

Vadlamudi R, Mandal M, Adam L, Steinbach G, Mendelsohn J, Kumar R. (1999). Regulation of cyclooxygenase-2 pathway by HER2 receptor. *Oncogene* **18**: 305–314.

Wang D, Dubois RN. (2006). Prostaglandins and cancer. *Gut* **55**: 115–122.

Wang D, Mann JR, DuBois RN. (2004). WNT and cyclooxygenase-2 cross-talk accelerates adenoma growth. *Cell Cycle* **3**: 1512–1515.

Wolff T, Rubin GM. (1998). Strabismus, a novel gene that regulates tissue polarity and cell fate decisions in *Drosophila*. *Development* **125**: 1149–1159.

Yao R, Natsume Y, Noda T. (2004). MAGI-3 is involved in the regulation of the JNK signaling pathway as a scaffold protein for frizzled and Ltap. *Oncogene* **23**: 6023–6030.

Zaric J, Ruegg C. (2005). Integrin-mediated adhesion and soluble ligand binding stabilize COX-2 protein levels in endothelial cells by inducing expression and preventing degradation. *J Biol Chem* **280**: 1077–1085.

Supplementary Information accompanies the paper on the Oncogene website (http://www.nature.com/onc)